Marine and Petroleum Geology 143 (2022) 105817

Contents lists available at ScienceDirect

Marine and Petroleum Geology

journal homepage: www.elsevier.com/locate/marpetgeo

Reconstruction of geochemical characteristics of original organic matter in drilling cuttings contaminated by oil-based mud

Liping Yuan [a,b,c], Wenmin Jiang [a,b,*], Yun Li [a,b], Rui Lei [d], Bin Cheng [a,b], Liangliang Wu [a,b], Yongqiang Xiong [a,b,**]

[a] State Key Laboratory of Organic Geochemistry, Guangzhou Institute of Geochemistry, Chinese Academy of Sciences, Guangzhou, 510640, China
[b] CAS Center for Excellence in Deep Earth Science, Guangzhou, 510640, China
[c] University of Chinese Academy of Sciences, Beijing, 100049, China
[d] Institute of Geography and Tourism, Guangdong University of Finance & Economics, Guangzhou, 510320, PR China

ARTICLE INFO

Keywords:
Oil-based drilling mud
Source rock
Catalytic hydropyrolysis
GC–IRMS
Bound bitumen

ABSTRACT

Oil-based drilling mud (OBM) contamination, commonly occurring in cuttings during petroleum exploration, has had been a problem seriously hindered source rock identification and evaluation. To eliminate the effect of contamination on "free" bitumen extracted directly from source rock, "enclosed" and "bound" bitumens were released from the mineral matrix by demineralization and from the kerogen structure using an improved catalytic hydropyrolysis technique, respectively. Geochemical and carbon isotopic compositions of the three types of bitumen were used to reconstruct the geochemical characteristics of original organic matter in their source rocks. Results indicate that "free" and "enclosed" bitumens have similar biomarker distributions and *n*-alkane $\delta^{13}C$ values in non-contaminated cuttings, but the former is more susceptible to OBM contamination. "Enclosed" bitumen can thus be used to characterize the organic geochemistry of source rocks contaminated by OBM. The carbon isotopic compositions of individual *n*-alkanes in "free" and "enclosed" bitumens differ from those in "bound" bitumen, likely because of the effects of diagenesis and other secondary alteration. "Bound" bitumen is more likely to preserve the molecular carbon isotopic characteristics of original organic matter in source rocks, while the "free" and "enclosed" bitumens more represent the generation products. Based on biomarker characteristics and carbon isotopic compositions of "bound" hydrocarbons, Wenchang (WC) Formation (Fm.) source rocks in the Zhu I Depression of the Pearl River Mouth Basin (PRMB) can be divided into three types in normal medium–deep (WC–I), shore–shallow (WC-II), and special medium–deep (with different algal blooms growth rates; WC-III) lacustrine source rocks. The special medium–deep lacustrine source rocks of Wenchang Fm. are characterized by high ratio of C_{30} 4-methylsteranes to C_{29} steranes (4-Me/C_{29} > 0.66) and heavy $\delta^{13}C$ values ($\delta^{13}C_{kerogen}$ < −26.1‰), which are obviously different from those of normal medium–deep lacustrine source rocks. The combination of "free", "enclosed", and "bound" hydrocarbons geochemical and isotopic compositions thus provides a comprehensive understanding of source rocks.

1. Introduction

Oil-based drilling mud (OBM) is a one of the tools during petroleum exploration, not only lubricating the drill bit but also carry large amounts of drilling material (e.g., drill cuttings and core) from the subsurface (Potts et al., 2019). Drill cuttings carred by drilling mud (e.g., OBM) from the subsurface have usually been used for oil–source correlations and source rock assessment, especially for deep- and ultra-deep-water petroleum exploration where core samples are usually scarce (Duarte et al., 2021; Jiang et al., 2021). However, OBM is usually a complex mixture of various additives (i.e., diesel, palm oil, oil-based esters, and their derivatives) that commonly wrapped the drill cuttings during drilling operations (McDermott, 1973; Caenn and Chillingar, 1996). It may percolate into the interior of cuttings and result in serious

* Corresponding author. State Key Laboratory of Organic Geochemistry, Guangzhou Institute of Geochemistry, Chinese Academy of Sciences, Guangzhou, 510640, China.
** Corresponding author. State Key Laboratory of Organic Geochemistry, Guangzhou Institute of Geochemistry, Chinese Academy of Sciences, Guangzhou, 510640, China.
E-mail addresses: jiangwm@gig.ac.cn (W. Jiang), xiongyq@gig.ac.cn (Y. Xiong).

https://doi.org/10.1016/j.marpetgeo.2022.105817
Received 4 February 2022; Received in revised form 9 June 2022; Accepted 10 June 2022
Available online 8 July 2022

contamination, possibly masking original organic geochemical information and hindering the assessment of source rocks (Petersen et al., 2017; Stuckman et al., 2019; Gabrielle and Irineu, 2021; Jiang et al., 2021). It is therefore a challenge to acquire original organic geochemical information from cuttings contaminated by OBM when the original, non-contaminated materials are absent.

OBM contamination has a significant influence on pyrolysis results, as identified in Rock–Eval pyrograms and the correlation between the basic indicators of Rock–Eval (Peters and Cassa, 1994; Jarvie, 2012; Carvajal-Ortiz and Gentzis, 2015; Rodriguez and Katz, 2021; Jiang et al., 2021). Cleaning the organic contaminates of surface of cuttings or core samples with organic solvents is necessary and solvent extraction is even used to eliminate the OBM contamination (Ratnayake and Sampei, 2019). Jiang et al. (2021) suggested that biomarkers and stable carbon isotopic compositions of "enclosed" bitumen are more reliable than those of "free" bitumen from drill cuttings contaminated by OBM and can be used to determine the organic geochemical characteristics of source rocks. In addition, Rullkötter and Michaelis (1990) indicated that the "enclosed" bitumen is less affected by contaminants (e.g., OBM) and secondary alteration (e.g., biodegradation and thermal maturation) than "free" bitumen. However, the underlying assumption of Jiang et al. (2021) was that "free" and "enclosed" bitumens would have similar geochemical and isotopic compositions in non-contaminated source rocks, and this needs to be verified.

Previous studies have indicated that "bound" bitumen obtained by catalytic hydropyrolysis (HyPy) is less affected by secondary alteration and preserves original information concerning macromolecular organic matter owing to the strong protective effect of the network structure of kerogens and oil asphaltenes (Love et al., 1995, 1997, 1998; Murray et al., 1998; Meredith et al., 2004, 2015, 2020). The HyPy technique has been widely applied in petroleum geochemistry, such as evaluation thermal maturity of organic matter (Love et al., 1996; Murray et al., 1998; Chen and Peng, 2017), investigation of reservoir charging history (Farrimond et al., 2003; Russell et al., 2004), and identification of the

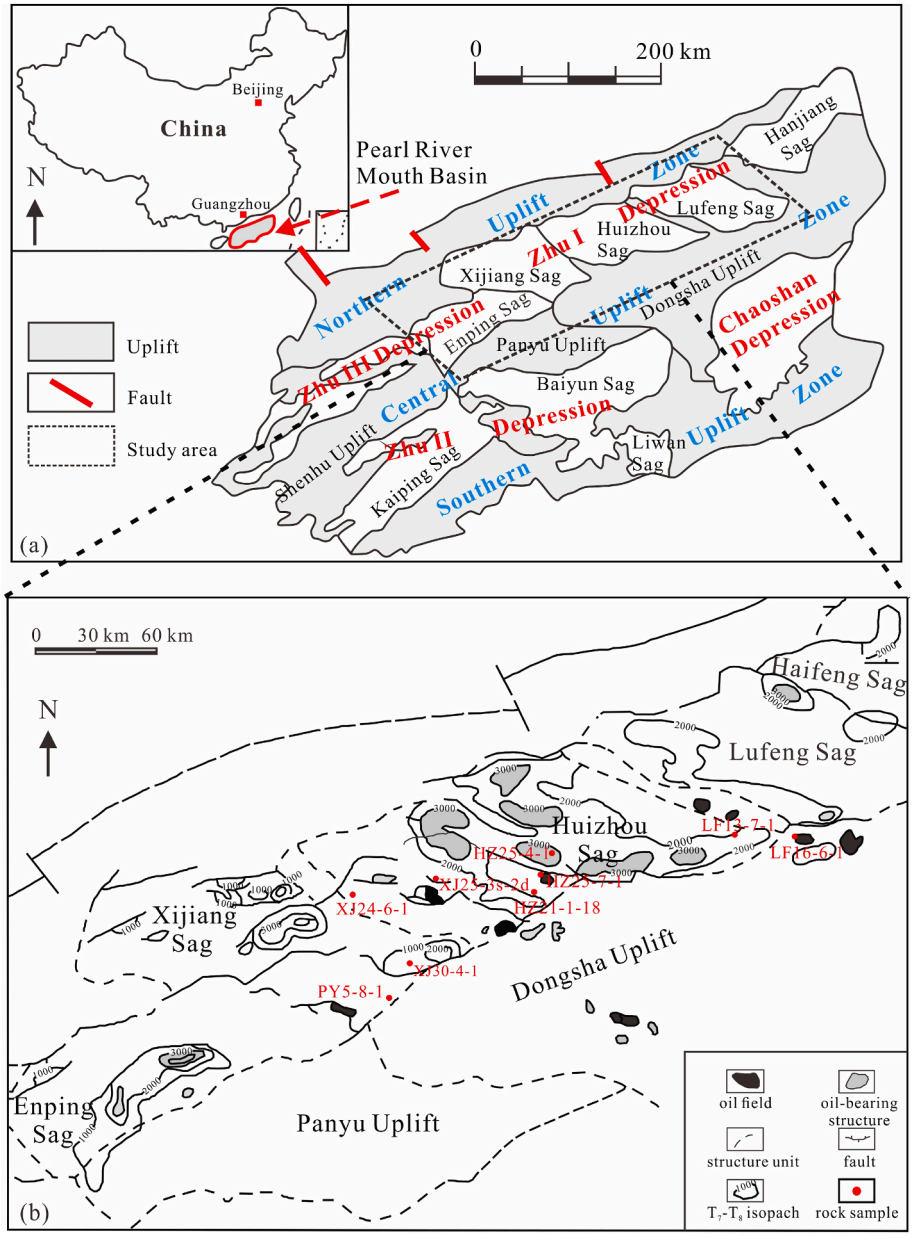

Fig. 1. (a) Location and division of first-order tectonic units of the Pearl River Mouth Basin (after Jiang et al., 2021). (b) Schematic geological map showing sampling locations in the Zhu I Depression (after Zhang et al., 2003).

origin of tar mats and pyrobitumens (Meredith et al., 2004). However, few studies have compared the geochemical and carbon isotopic compositions of "free", "enclosed", and "bound" bitumens from source rocks. Our previous study indicated that improved HyPy technique effectively eliminates the adverse effect of OBM on drilling cuttings and can be used to reconstruct the source and sedimentary environment of indigenous organic matter in the main source rocks of the Baiyun deep-water area of the Pearl River Mouth Basin (PRMB; Yuan et al., 2021). However, "bound" biomarkers were not investigated in that study due to their relatively low abundance, with only the carbon isotopic compositions of individual *n*-alkanes covalently bound to kerogen frameworks being considered.

The PRMB has become a "hot spot" for petroleum exploration, with a series of oil and gas fields and oil- and gas-bearing structures being discovered over the last 30 years (Fig. 1; Chen and Pei, 1993; Robison et al., 1998; Shi et al., 2014; Fu et al., 2019, 2020). The Eocene Wenchang Fm. is an important source rock which is the predominant origin for the discovered petroleum and widely distributed in different sags of the PRMB (Fu et al., 2001; Huang et al., 2003; Bao et al., 2017; Jiang et al., 2021). As the absent of core samples, which are much less prone to OBM contamination, the drill cutting samples from the Wenchang Fm. in the Zhu I Depression of the PRMB were taken as substitutes, and the "free", "enclosed", and "bound" bitumens within them were investigated. The main objective was to make a full understanding of the organic geochemistry of source rocks by comparing the biomarkers and carbon isotopic compositions among the three types of bitumen, and to provide a method for reconstruction of the geochemical characteristics of source rocks contaminated by OBM.

2. Geological background

The PRMB, with an area of 1.75×10^5 km^2, located on the northern continental shelf of the South China Sea (Fig. 1) and developed on the Caledonian and Hercynian fold basement (Chen and Pei, 1993), is one of the important petroliferous Mesozoic–Cenozoic sedimentary basins in the China (Li and Rao, 1994; Robison et al., 1998). It is composed of five tectonic units from south to north, namely, the Southern Uplift, Southern Depression, Central Uplift, Northern Depression and Northern step-fault zones. Each tectonic unit is consisted of several sags and uplifts (Chen and Pei, 1993). The Zhu I Depression with an exploration area of 4.2×10^4 km^2 is located in shallow-water area in the Northern Depression of PRMB, displaying a NE-SW trending direction (Fig. 1; Niu et al., 2019), comprised of several hydrocarbon-rich sags, such as Lufeng, Huizhou, Xijiang, and Enping sags (Zhang et al., 2003; Peng et al., 2016).

Zhu I Depression has experienced three tectonic evolutions, including rifting, fault-sag transition and depression, resulting in a dual configuration of the early rifting to the post-rift subsidence and the early nonmarine facies to the late marine facies (Robison et al., 1998; Shi et al., 2014). The stratigraphy of the Zhu I Depression is recognized as Eocene Wenchang and Enping formations, Oligeocene Zhuhai Fm., Miocene Zhujiang, Hanjiang, and Yuehai formations, Pliocene Wanshan Fm., and Quaternary strata from bottom to top (Fig. 2). The continental sedimentary basin is mainly deposited during the rifting period, in which Wenchang and Enping formations had been widely deposited. The marine strata of Zhuhai, Zhujiang, Hanjiang, Yuehai, and Wanshan are primarily formed in the subsidence stage (Zhang et al., 2003; Shi et al., 2014; Peng et al., 2016). The Wenchang and Enping formations are two effective petroleum source rocks in the Zhu I Depression (Hu et al., 2015). The Wenchang Fm., mainly developed medium–deep lacustrine or shore-shallow lacustrine mudstones, consisting of grey to black lacustrine mudstones with thin sandstones and siltstones, is the main source of the most of discovered oils in the Zhu I Depression (Huang et al., 2003; Zhang et al., 2003; Fu and Zhu, 2007). The Zhuhai and the Zhujiang formations are major reservoirs consisted of sandstone and reef limestone types. With regards the petroleum system elements,

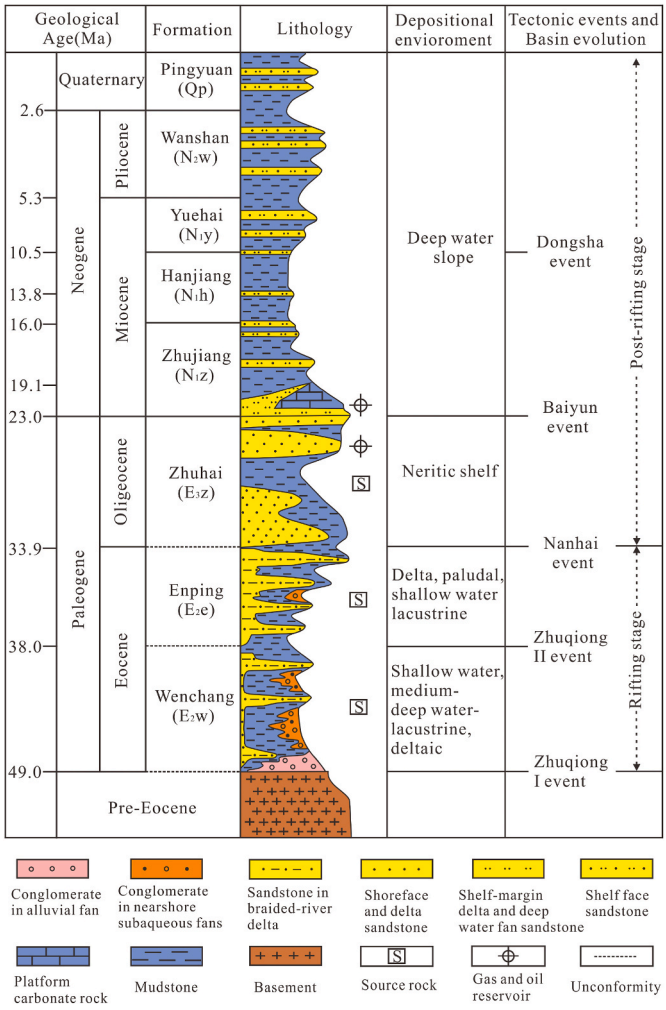

Fig. 2. Stratigraphy of the Zhu I depression in the Pearl River Mouth basin (after Ping et al., 2019).

the Hanjiang Fm. mainly serves as regional cap rocks, composed of prodelta and shelf shales (Shi et al., 2014; Hu et al., 2015).

3. Samples and methods

3.1. Samples and sample preparation

Nine cutting samples with relatively high total organic carbon (TOC) contents (>0.5 wt%) were collected from the Eocene Wenchang Fm. in the depth interval 3600–4600 m in the Zhu I Depression (Fig. 1). Sample details are provided in Table 1. The samples were washed using deionized water to remove surface contamination (e.g., OBM), air-dried naturally, crushed, and ground to powder (120 mesh). The TOC contents of powdered samples (~100 mg) were determined using a Leco-230 C/S analyzer. An IFP Rock–Eval VI instrument was applied to pyrolysis of source rock samples before and after the "free" bitumen extraction (Lafargue et al., 1998; Behar et al., 2001). The powdered samples were weighed and put in a small crucible. The programmed temperature of pyrolysis is initially held at 300 °C for 3 min, then ramped to 650 °C at 25 °C/min and holding at 650 °C for 3 min. The oxidation program was kept in 300 °C for 1 min, then heated to 850 °C at 20 °C/min, held isothermal for 5 min at 850 °C. A Soxhlet apparatus was used to extract soluble organic matter from pulverized samples using a mixed dichloromethane/methanol (93/7, v/v) solvent to obtain "free" bitumen. The extracted residues were demineralized by conventional acid demineralization to prepare kerogen concentrates (Jiang et al.,

Table 1
Total organic carbon (TOC) content, Rock–Eval parameters and kerogen carbon isotopes of source rocks in the Zhu I Depression, PRMB.

Sample No.	Well	Formation	Depth(m)	$\delta^{13}C_{kerogen}$ (‰)	Before extraction						After extraction					
					TOC	S_1	S_2	T_{max}	HI	PI	TOC	S_1	S_2	T_{max}	HI	PI
1	LF13-7-1	Wenchang	3680–3694	−26.4	2.64	3.31	10.97	435	416	0.23	2.28	0.90	7.23	438	317	0.11
2	LF13-7-1	Wenchang	3709–3730	−25.9	3.10	3.98	13.47	438	435	0.23	2.70	0.88	9.14	439	339	0.09
3	LF16-6-1	Wenchang	3250–3275	−26.0	1.74	0.86	9.32	432	536	0.08	1.51	0.60	9.00	434	596	0.07
4	HZ21-1-18	Wenchang	4220–4250	−27.3	0.88	0.32	1.89	338	215	0.14	0.82	0.07	1.19	448	145	0.06
5	HZ25-4-1	Wenchang	3760–3780	−26.1	2.29	0.66	8.26	445	361	0.07	2.07	0.04	6.53	445	315	0.01
6	HZ25-7-1	Wenchang	3855–3865	−23.9	3.16	1.18	13.13	444	416	0.08	3.00	0.09	10.35	444	345	0.01
7	XJ24-3s-2d	Wenchang	4444–4450	−27.7	1.23	0.63	3.48	426	283	0.15	0.80	0.21	2.03	433	254	0.09
8	XJ24-6-1	Wenchang	4550–4580	−27.6	1.90	0.91	3.80	445	200	0.19	1.51	0.22	2.95	452	195	0.07
9	PY5-8-1	Wenchang	3678–3694	−27.1	2.44	0.66	10.73	442	440	0.06	2.17	0.11	9.06	445	418	0.01

Note: $\delta^{13}C_{kerogen}$ means $\delta^{13}C$ values of extracted kerogen; TOC is in "wt.%", S_1 means free hydrocarbons; S_2 means pyrolytic hydrocarbons; S_1 and S_2 are in "mg HC/g rock"; T_{max} is in "°C"; HI = $S_2 \times 100$/TOC, in "mg HC/g TOC"; PI = $S_1/(S_1+S_2)$.

2021). The kerogens were treated with a benzene/acetone/methanol mixture (5/5/2, v/v/v) for 14 d to extract organic matter trapped in or adsorbed on the kerogen matrix ("enclosed" bitumen). Activated copper granules were used to remove inorganic sulfur during each extraction.

3.2. Stable carbon isotope analyses

The $\delta^{13}C_{kerogen}$ values of extracted kerogen samples were determined using a C/N/S Analyzer (CE EA 1112) (converting organic carbon into CO_2 at 960 °C) combined with a Thermo Finnigan Delta Plus XL mass spectrometer. The $\delta^{13}C$ values of extracted kerogen are reported relative to the Vienna Peedee Dee Belemnite (VPDB) standard. Each sample was measured at least twice with an analytical precision of better than ±0.3‰, and the average of two or more runs reported as the final result.

3.3. Improved catalytic hydropyrolysis

Our previous study has demonstrated that the OBM contamination could penetrate to the interior of drilling cuttings, influencing their kerogen catalytic hydropyrolysates, and the off-line vacuum degassing can effectively eliminate hydrocarbon contaminants in the kerogen catalytic hydropyrolysates (Yuan et al., 2021). A high-vacuum (<10 mm Hg) degassing system (Micromeritics VacPrep 061) was used for off-line degassing of extracted kerogen. The extracted kerogen powders were placed in quartz-glass tubes connected to the instrument, heated at 250 °C for 24 h, and cooled to ambient temperature for HyPy.

The degassed kerogens were macerated in an aqueous/methanol solution of ammonium dioxydithiomolybdate ($(NH_4)_2MoO_2S_2$) to give a nominal loading of 5 wt% Mo, and freeze-dried under vacuum for HyPy experiments involving three steps as follows. To remove system background contamination, a blank program was run before each sample loading by heating the reactor rapidly (at 300 °C min^{-1}) from ambient temperature to 550 °C and holding for 5 min. Blank products were trapped on silica gel in a liquid-nitrogen (LN2) cold-trap. The sample was then loaded in the reactor and clean silica gel placed in the collection trap. Thermal desorption was initiated by heating from ambient temperature to 250 °C at 250 °C min^{-1}, then to 300 °C at 20 °C min^{-1}, and holding at 300 °C for 5 min to obtain adsorbed and weakly covalently bound components. The collection trap was then replaced, and HyPy was employed to release the more strongly covalently bound compounds, with a temperature program from ambient temperature to 250 °C at 300 °C min^{-1}, to 520 °C at 8 °C min^{-1}, and maintained at 520 °C for 5 min. In all processes, hydrogen, as protective, reaction, and carrier gas, was maintained at 15 MPa with a flow rate of 5 dm^3 min^{-1} to ensure that all products were swept quickly into the LN2-cooled cold-trap. The recovered method of "free" bitumen was also used to collect hydropyrolysates ("bound" bitumen) absorbed on the silica gel. The details of HyPy procedure were described by Chen and Peng (2017).

3.4. GC–MS and GC–IRMS analyses

After being deasphaltened by *n*-hexane precipitation, the "free", "enclosed", and "bound" bitumens, which were Soxhlet extracted from "initial" cuttings, kerogen, and hydropyrolysates, respectively, were separated into saturated, aromatic, and resin fractions using a silica–alumina column (3:1 v/v) with successive elution in *n*-hexane, *n*-hexane/dichloromethane (3:2, v/v), and methanol, respectively. Saturated fractions were analyzed by gas chromatography–mass spectrometry (GC–MS) and gas chromatography–isotope ratio mass spectrometry (GC–IRMS).

GC–MS analysis of the saturated fractions involved an Agilent 7890A GC coupled to a 5977 MS equipped with a 60 m × 0.25 mm i.d. × 0.25 μm film-thickness HP-1MS column. A constant-flow mode with a flow rate of 1.2 mL min^{-1} of carrier gas (ultrahigh purity He) and splitless injection mode at 300 °C were employed. The MS was operated in electron-ionization mode at 70 eV. The GC oven temperature was programed to 80 °C for 2 min, ramped at 6 °C min^{-1} to 190 °C, held for 2 min, ramped to 290 °C at 3 °C min^{-1}, and held for 30 min. The selected-ion monitoring mode was used for saturated fractions, including *m/z* 85 for *n*-alkanes, *m/z* 191 for terpanes, *m/z* 217 for steranes, and *m/z* 412 for bicadinanes, which are the base peaks for each types of biomarkers, respectively.

After GC–MS analysis, iso- and cyclic alkanes in saturated fractions were further removed by urea adduction to provide *n*-alkanes. Stable carbon isotopic compositions of *n*-alkanes were determined using an Elementar isoprime visION IRMS interfaced with an Agilent 7890B GC fitted with a 60 m × 0.25 mm i.d. × 0.25 μm film-thickness HP-1MS column. The GC oven temperature was held at 60 °C for 2 min, ramped to 150 °C at 15 °C min^{-1}, to 300 °C at 3 °C min^{-1}, and held for 20 min. A constant-flow mode with a flow rate of 1.0 mL min^{-1} of carrier gas (ultrahigh purity He) and a split mode with a split ratio of 5:1 at 300 °C were employed. The combustion furnace was run at 950 °C. A standard mixture of *n*-alkanes (nC_{12}, nC_{14}, nC_{16}, nC_{18}, nC_{20}, nC_{22}, nC_{25}, nC_{28}, nC_{30}, nC_{32}, and nC_{35}) of known carbon isotopic composition was analyzed daily before the samples to monitor instrument stability, and each sample was analyzed at least twice with average values being reported. Reproducibility was generally within ±0.3‰. $\delta^{13}C$ values are reported in per mil (‰) relative to the VPDB standard.

4. Results

TOC contents and Rock–Eval parameters of the studied Wenchang Fm. source rocks are listed in Table 1. The TOC contents, S_2, T_{max}, hydrogen index (HI), and production index (PI) values for the unextracted samples are in the ranges of 0.88–3.16 wt%, 1.89–13.47 mg hydrocarbon (HC) g^{-1} rock, 338–445 °C, 200–536 mg HC g^{-1} TOC, and 0.07–0.23, respectively (Table 1). For extracted samples, the values of TOC, S_2, T_{max}, HI, and PI range from 0.80 to 3.00 wt%, 1.19–10.35 mg hydrocarbon (HC) g^{-1} rock, 433–452 °C, 145–596 mg HC g^{-1} TOC, and

0.01–0.11, respectively. The $\delta^{13}C_{kerogen}$ values range from −27.7‰ to −23.9‰ (Table 1).

Selected molecular parameters of the samples studied here are listed in Table 2. The carbon preference index (CPI) values range from 0.89 to 1.40 (median 1.05). The ratios of pristine/phytane (Pr/Ph) for the "free" and "enclosed" saturated hydrocarbons are in the range of 1.19–4.95 (median 1.94) and 0.65–1.61(median 1.05), respectively. Pr and Ph are hardly detectable in the "bound" saturated hydrocarbons. The C_{21-}/C_{22+}, C_{30} 4-methylsteranes/C_{29} steranes (4-Me/C_{29}), bicadinane-T/C_{30} hopanes (T/C_{30}H), C_{21}/C_{23} tricyclic terpanes (C_{21}/C_{23}TT), $(C_{19} + C_{20})/C_{23}$ tricyclic terpanes [$(C_{19} + C_{20})/C_{23}$TT] and C_{35}-homohopane index (C_{35}H/C_{34}H 22S) ratios range from 0.3 to 2.94 (median 0.7), 0.02 to 1.38 (median 0.14), 0.01 to 1.7 (median 0.32), 0.38 to 2.23 (median 1.10), 0.19 to 5.06 (median 1.18), and respectively. The ratios of 20S/(20S + 20R) and αββ/(ααα + αββ) for the C_{29} steranes are between 0.08–0.68 and 0.12–0.85, respectively.

The $\delta^{13}C$ values of individual *n*-alkanes for these samples are listed in Table 3. The $\delta^{13}C$ values of individual *n*-alkanes for "free", "enclosed", and "bound" bitumens range from −32.3‰ to −25.9‰, −32.4‰ to −27.6‰, and −32.3‰ to −22.1‰, respectively.

5. Discussion

5.1. Preliminary identification of OBM contamination

As cutting samples are easily subjected to drilling mud contamination, especially in offshore exploration because of common application of OBM (Petersen et al., 2017; Jiang et al., 2021; Yuan et al., 2021), it is necessary to determine whether studied samples are contaminated prior to further analysis. Based on Rock–Eval results and distribution of saturated hydrocarbons, Petersen et al. (2017) demonstrated that OBM contamination could result in high PI values and abnormal distributions of saturated hydrocarbons with low carbon numbers (nC_{11}–nC_{14}). Rock–Eval pyrograms and parameters obtained from source rock analysis before and after extraction are widely used to determine whether samples are contaminated by drilling mud (particularly oil-based mud; Peters and Cassa, 1994; Jarvie, 2012; Carvajal-Ortiz and Gentzis, 2015; Petersen et al., 2017). The OBM contaminated samples usually have a prominent shoulder on the S_2 peak (light and migrated hydrocarbons) and relatively high PI values at relative low maturity (generally >0.1; Carvajal-Ortiz and Gentzis, 2015; Petersen et al., 2017; Jiang et al., 2021). Fig. 3 shows the Rock–Eval pyrograms for the nine cutting samples before and after extraction. Before extraction, samples 1, 2, 4, 7, and 8 have a prominent shoulder on the S_2 peak (especially for 2, 4, and 8), which is not found in samples 3, 5, 6, and 9 (Fig. 3a). Some unextracted samples (i.e., 4 and 7) have relatively low T_{max} (<435 °C) but high PI values (>0.1) (Fig. 4), which may imply OBM contamination in these samples (Petersen et al., 2017). Additionally, abnormal distributions of saturated hydrocarbons with low carbon numbers were also existed in the extracts ("free" bitumen) of samples 1, 2, 4, 7, and 8, and were not evident for the samples 3, 5, 6, and 9 (Fig. 5), indicating the possible contamination of extraneous hydrocarbons for the former samples (Petersen et al., 2017; Jiang et al., 2021). Hence, we speculated that cutting samples 1, 2, 4, 7, and 8 were contaminated by OBM, and samples 3, 5, 6, and 9 were not contaminated mainly based on the Rock–Eval results and the distributions of saturated hydrocarbons (Table 1; Figs. 3 and 4).

As showing in Fig. 3b, the solvent extraction not only effectively eliminates OBM contamination (shoulder on the S_2 peak of samples 2, 4, and 8), but also removes S_1 hydrocarbons. Thus, the S_1 and PI values become unreliable for extracted samples. Considering the same pretreatment for contaminated and uncontaminated samples, the other Rock–Eval parameters (i.e., S_2, HI, and T_{max}) of all the extracted cutting samples are used to assess source rock quality (Petersen et al., 2017; Jiang et al., 2021). As showing in Fig. 5a, TOC and S_2 values of the extracted samples are in the ranges of 0.8–3.0 wt% and 1.19–10.35 mg HC g^{-1} rock, respectively, indicating a relatively high organic abundance and hydrocarbon generation potential, which is consistent with previous studies that the organic matter in Wenchang Fm. source rocks is hydrogen rich and oil prone (Chen et al., 1991; Huang, 1998; Shi et al., 2011; Bao et al., 2017). T_{max} and HI values are in the ranges of 433–452 °C and 145–596 mg HC g^{-1} TOC, respectively, suggesting that the most samples are in the mature stage with vitrinite reflectance (R_o) of 0.5–1.0% and contain type II_1 kerogen with an indefinite proportion of type I and II_2 kerogens, which is also consistent with previous studies (Fu and Zhu, 2007; Shi et al., 2014; Jiang et al., 2015; Niu et al., 2019).

5.2. Molecular composition characteristics of "free", "enclosed", and "bound" bitumens

5.2.1. Biomarker distribution

5.2.1.1. n-Alkanes and acyclic isoprenoids. For uncontaminated samples 3, 5, 6, and 9, the total ion chromatogram (TIC) of saturated hydrocarbons in "free" bitumen and corresponding "enclosed" bitumen are generally similar (Fig. 6). For example, the *n*-alkanes of "free" and "enclosed" bitumens in samples 5, 6, and 9 range mainly between nC_{14} and nC_{29}, with a unimodal distribution dominated by middle–long chain *n*-alkanes (nC_{22}–nC_{30}), whereas the *n*-alkanes of "free" and "enclosed" bitumens in sample 3 display a bimodal distribution with maxima at nC_{15} and nC_{25}. In addition, the CPI values of "free" and "enclosed" saturated hydrocarbons are generally near 1.0 (except for sample 3), ranging from 0.96 to 1.19 (median 1.05), indicating that these source rock samples have reached a mature stage, which is consistent with their high T_{max} values (444–445 °C). However, the CPI value of "free" saturated hydrocarbons in sample 3 (CPI = 1.4) is higher than that of the corresponding "enclosed" saturated hydrocarbons, with an evident odd–even carbon number preference, indicating low maturity, which is consistent with its lower maturity, i.e., T_{max} = 434 °C; C_{29} 20S/(20S + 20R) and C_{29} αββ/(ααα + αββ) are 0.27 and 0.28, respectively, which is approximately corresponding to 0.6–0.65% Ro (Seifert and Moldowan, 1980). For uncontaminated samples, most "free" and "enclosed" saturated hydrocarbons have relatively low pristine/phytane (Pr/Ph) ratios (<2; Table 2), suggesting that they were deposited in an anoxic to suboxic sedimentary environment (Didyk et al., 1978; Powell, 1988).

The gas chromatograms of saturated hydrocarbon fractions in "bound" bitumen of uncontaminated samples generally differ from those of the corresponding "free" and "enclosed" bitumens (Fig. 6). For example, "bound" bitumens in samples 5, 6, and 9 have a wider carbon number range (nC_{13}–nC_{36}) that is dominated by short–middle chain *n*-alkanes, with higher nC_{21-}/nC_{22+} ratios than those of "free" and "enclosed" bitumens. This may be attributed to the protective effect of the macromolecular network structure of kerogen on covalently bound molecules, which results in "bound" bitumen being less affected by diagenetic processes and secondary alteration (Love et al., 1995, 1998; Murray et al., 1998; Russell et al., 2004; Liao et al., 2012). The *n*-alkanes of the three types of bitumen in sample 3 have similar bimodal distributions, indicating that it has not been subjected to a high degree of diagenetic and/or secondary alteration, as supported by its low maturity. Pristane and phytane are conspicuously less abundant in or absent from "bound" bitumen, possibly because they are the products of late diagenesis, or their precursors were few or not integrated into the kerogen network structure during sedimentary diagenesis (Blumer and Thomas, 1965; Brooks and Smith, 1969; Wang et al., 2012). Therefore, the following discussion is based on data for acyclic isoprenoids from "enclosed" bitumen and/or "free" bitumen.

For contaminated samples 1, 2, 4, 7, and 8, the gas chromatograms of "free" bitumen differ from those of the corresponding "enclosed" bitumen. Saturated hydrocarbons in "free" bitumen display a small unresolved complex mixture (of mainly low-molecular-weight *n*-alkanes), similar to that of oil-based mud filtrate (Fig. 6; Jiang et al., 2021;

Table 2
Biomarker parameters in the "free", "enclosed", and "bound" bitumens.

	Sample No.	Contaminated	$\delta^{13}C_{Av\text{-}alkanes}$ (‰)	Pr/Ph	C_{21-}/C_{22+}	CPI	$C_{21}/C_{23}TT$	$(C_{19}+C_{20})/C_{23}$ TT	$C_{35}H/C_{34}H$ 22S	$T/C_{30}H$	4-Me/C_{29}	C_{27}(%)	C_{28}(%)	C_{29}(%)	20S	20ββ
"free" bitumen	1	Yes	−28.6	1.89	0.59	1.03	1.44	1.18	0.57	0.09	0.06	8	38	54	0.66	0.85
	2	Yes	−27.5	1.92	0.53	1.09	1.34	1.51	0.48	0.19	0.37	56	5	38	0.34	0.32
	3	No	−30.3	3.19	0.44	1.40	1.60	2.14	–	0.03	0.18	37	25	38	0.27	0.28
	4	Yes	−30.8	2.53	0.82	1.03	0.59	0.86	0.70	1.70	0.14	29	26	45	0.65	0.46
	5	No	−30.0	1.82	0.58	1.06	1.61	2.65	0.53	1.64	1.38	35	18	46	0.68	0.25
	6	No	−27.3	1.94	0.70	1.08	1.50	1.93	0.50	0.93	1.05	29	21	50	0.64	0.29
	7	Yes	−30.4	4.95	0.85	1.27	0.38	0.66	0.56	0.60	0.06	13	22	65	0.35	0.29
	8	Yes	−30.2	2.65	1.41	1.02	0.51	0.67	0.67	0.32	0.05	32	27	41	0.43	0.34
	9	No	−31.0	1.19	0.48	1.04	0.88	0.54	0.58	0.02	0.52	23	24	53	0.63	0.39
"enclosed" bitumen	1	Yes	−29.0	0.73	0.40	1.05	0.73	0.19	0.48	0.13	0.11	37	21	41	0.65	0.38
	2	Yes	−27.9	0.69	0.43	1.09	0.72	0.25	0.52	0.33	0.15	29	24	47	0.50	0.29
	3	No	−30.1	1.05	0.60	1.00	0.58	0.52	–	0.05	0.10	39	24	37	0.42	0.35
	4	Yes	−30.3	1.05	0.88	1.07	0.81	0.55	0.62	1.13	0.08	30	27	43	0.48	0.41
	5	No	−29.6	1.07	0.46	1.05	0.52	0.45	0.52	0.86	0.31	36	32	32	0.55	0.37
	6	No	−28.5	0.93	0.36	0.96	0.49	0.36	0.53	0.67	0.24	37	29	34	0.49	0.38
	7	Yes	−29.6	0.65	0.45	0.89	0.57	0.41	0.48	0.23	0.08	31	26	43	0.41	0.35
	8	Yes	−30.3	1.61	0.55	1.15	0.46	0.55	0.70	0.47	0.07	31	29	40	0.47	0.40
	9	No	−31.1	1.05	0.30	1.19	0.61	0.44	0.72	0.04	0.20	35	26	39	0.55	0.37
"bound" bitumen	1	Yes	−26.8	–	1.24	1.01	1.25	1.61	0.58	0.11	0.14	37	26	37	0.45	0.37
	2	Yes	−26.0	–	1.02	1.01	1.53	3.05	0.70	0.17	0.22	41	24	35	0.43	0.21
	3	No	−28.4	–	0.79	1.07	1.66	3.68	0.30	0.01	0.09	42	17	41	0.08	0.12
	4	Yes	−28.5	–	2.24	1.18	1.22	2.90	0.82	1.01	0.04	16	19	64	0.21	0.36
	5	No	−28.5	–	1.34	1.02	1.10	1.43	0.68	0.77	0.77	28	27	45	0.51	0.41
	6	No	−24.4	–	1.49	0.99	1.81	1.59	0.70	0.75	0.66	30	20	50	0.29	0.57
	7	Yes	−28.6	–	1.06	0.99	1.26	5.06	0.54	0.29	0.10	16	11	73	0.33	0.24
	8	Yes	−28.3	–	2.94	1.39	1.10	4.39	0.34	0.61	0.02	13	23	63	0.47	0.47
	9	No	−31.6	–	0.84	1.02	2.23	2.44	0.84	0.07	0.26	36	27	37	0.33	0.14

Note: $\delta^{13}C_{Av\text{-}alkanes}$ means arithmetic mean for the carbon isotopes of individual hydrocarbons; Pr/Ph = pristane/phytane; Pr/nC_{17} = pristane/n-C_{17}; Ph/nC_{18} = phytane/n-C_{18}; $CPI = \frac{(\sum_{i=n}^{m} C_{2i+1}) + (\sum_{i=n+1}^{m+1} C_{2i+1})}{2\cdot(\sum_{i=n+1}^{m+1} C_{2i})}$ (Marzi et al., 1993), where n is the number of carbons in the initial normal alkane divided by 2, m is the number of carbons in the final normal alkane divided by 2, and i is an exponent, n = 10 and m = 14; $C_{21}/C_{23}TT = C_{21}/C_{23}$ tricyclic terpanes; $(C_{19} + C_{20})/C_{23}TT = (C_{19} + C_{20})/C_{23}$ tetracyclic terpanes; $C_{35}H/C_{34}H$ 22S = C_{35}/C_{34}-17αt(H),21β(H) 22S Homohopanes; $T/C_{30}H$ = bicadinane-T/C_{30} hopane (calculated from m/z 412); C_i (%): C_i Regular steranes/($C_{27} + C_{28} + C_{29}$) Regular steranes; 4-Me/C_{29} = C_{30} 4-methylsteranes/C_{29} steranes (calculated from m/z 217); 20S: 20S/(20S + 20R) C_{29} sterane ratio; 20ββ: αββ/(ααα + αββ) C_{29} sterane ratio; "–" means no data.

Table 3
Stable carbon isotopic compositions of individual *n*-alkanes for "free", "enclosed", and "bound" bitumens ($\delta^{13}C$, ‰, VPDB).

	Sample No.	C_{13}	C_{14}	C_{15}	C_{16}	C_{17}	C_{18}	C_{19}	C_{20}	C_{21}	C_{22}	C_{23}	C_{24}	C_{25}	C_{26}	C_{27}	C_{28}	C_{29}	C_{30}	C_{31}	C_{32}	C_{33}	C_{34}	C_{35}
"free" bitumen	1		−26.9	−27.1	−27.7	−28.2	−28.6	−28.9	−29.2	−29.1	−29.2	−29.0	−28.7	−28.6	−28.6	−28.7	−28.6	−28.7	−28.7	−28.9	−28.2	−28.5	−29.5	−28.5
	2			−26.5	−27.2	−27.4	−27.8	−27.8	−27.9	−27.9	−27.7	−27.5	−27.2	−27.2	−27.1	−27.2	−27.4	−27.2	−27.4	−27.8	−27.2	−27.5	−28.4	
	3			−27.6	−28.0	−28.4	−29.5	−30.2	−30.8	−31.6	−31.0	−31.0	−30.8	−30.7	−30.6	−30.6	−30.4	−30.4	−30.5	−31.2	−30.1	−31.9		
	4				−29.4	−30.5	−30.5	−31.2	−31.2	−31.5	−31.2	−31.1	−30.8	−31.0	−30.7	−31.0	−30.7	−30.8	−30.9	−30.8				
	5			−28.4	−28.4	−29.5	−29.9	−30.7	−30.8	−31.3	−30.7	−30.9	−30.2	−30.2	−29.9	−30.1	−29.7	−29.7	−29.8	−30.2	−29.4	−29.7	−30.2	
	6			−25.9	−26.3	−26.1	−26.2	−26.6	−26.7	−27.1	−27.2	−27.6	−27.6	−27.8	−27.7	−27.8	−28.2	−27.8	−27.8	−28.3	−27.6	−28.1	−27.5	
	7				−30.2	−31.1	−31.6	−31.0	−30.1	−30.5	−30.3	−30.1	−29.7	−29.6	−29.5	−29.8	−31.1							
	8		−28.6	−29.1	−29.2	−29.5	−29.7	−30.0	−30.0	−30.1	−30.0	−30.2	−30.2	−30.5	−30.5	−30.9	−30.8	−31.1	−31.4	−32.0				
	9			−28.5	−28.7	−29.9	−31.7	−31.6	−31.9	−32.3	−31.8	−31.7	−31.2	−31.3	−31.2	−32.0	−31.3	−31.5	−31.0	−30.5	−30.4	−31.0		
"enclosed" bitumen	1				−28.8	−28.8	−28.8	−28.8	−28.7	−28.9	−29.0	−29.2	−28.9	−29.0	−28.9	−29.1	−29.2	−29.2	−29.2	−29.3				
	2				−27.6	−27.8	−28.3	−28.2	−28.1	−28.0	−27.9	−28.0	−27.6	−27.7	−27.6	−28.0	−27.9	−27.9	−27.9	−27.6	−27.8	−28.4		
	3				−29.8	−30.1	−29.8	−30.1	−29.7	−30.0	−30.2	−30.5	−30.3	−30.2	−29.9	−30.3	−30.4	−30.0	−30.4	−29.3	−30.0	−30.6		
	4					−30.1	−29.9	−30.7	−30.6	−31.3	−30.7	−30.8	−30.2	−30.3	−30.2	−30.9	−28.6	−29.1						
	5				−28.3	−29.2	−29.0	−29.7	−29.8	−30.0	−30.0	−30.4	−29.9	−29.8	−29.6	−29.7	−29.7	−30.1						
	6					−28.1	−28.0	−28.0	−27.7	−27.7	−28.8	−28.7	−28.6	−28.6	−28.5	−28.7	−28.8	−29.8						
	7					−29.4	−29.2	−29.6	−29.3	−29.9	−30.4	−30.5	−29.9	−29.9	−29.8	−29.9	−28.5	−28.2	−29.7	−29.1				
	8				−29.2	−29.6	−29.8	−29.9	−29.9	−30.1	−30.1	−30.2	−30.2	−30.6	−30.4	−31.1	−31.2	−32.4						
	9					−29.5	−29.9	−30.7	−30.9	−31.4	−31.6	−31.8	−31.2	−31.4	−31.3	−31.7	−31.1	−31.3	−31.7					
"bound" bitumen	1	−25.1	−25.4	−25.6	−26.0	−26.2	−26.5	−26.9	−26.9	−26.9	−26.8	−26.9	−27.1	−26.9	−27.2	−27.3	−27.4	−27.5	−27.6	−27.6	−27.4	−27.4	−27.9	
	2	−24.8	−25.2	−25.4	−25.6	−25.6	−25.6	−25.7	−25.8	−25.9	−25.7	−25.7	−25.8	−26.1	−26.1	−26.0	−26.8	−26.7	−26.4	−27.0	−26.1	−26.3	−26.8	
	3	−26.1	−26.4	−26.8	−27.3	−27.9	−28.3	−28.9	−29.2	−29.5	−29.1	−29.3	−29.2	−29.0	−29.4	−28.7	−29.0	−28.9	−28.3	−29.0	−28.3	−28.2	−28.0	
	4			−28.3	−27.9	−28.0	−27.8	−28.8	−29.0	−28.7	−29.1	−28.5	−28.9	−28.7	−28.6									
	5		−26.5	−27.8	−28.1	−28.5	−28.5	−28.8	−29.1	−29.3	−28.8	−28.9	−28.5	−28.8	−29.0	−28.5	−28.8	−28.4	−28.6	−28.8	−28.3	−28.2	−28.7	
	6	−22.1	−22.4	−23.0	−23.5	−23.8	−24.1	−24.2	−24.1	−24.2	−24.3	−24.3	−24.4	−24.5	−24.4	−25.1	−25.3	−25.4	−25.6	−25.7	−25.3	−25.4	−25.6	
	7			−27.8	−28.0	−28.1	−28.5	−28.7	−28.8	−28.4	−28.7	−28.4	−28.8	−28.8	−28.8	−28.7	−28.7	−29.7						
	8					−27.7	−27.6	−28.3	−27.6	−28.1	−29.0	−28.6	−28.8	−28.8	−28.9									
	9	−29.7	−30.4	−30.6	−31.1	−31.4	−31.5	−31.7	−31.8	−32.0	−32.1	−32.1	−32.2	−32.3	−32.1	−31.9	−32.1	−31.9	−31.8	−31.3	−31.9			

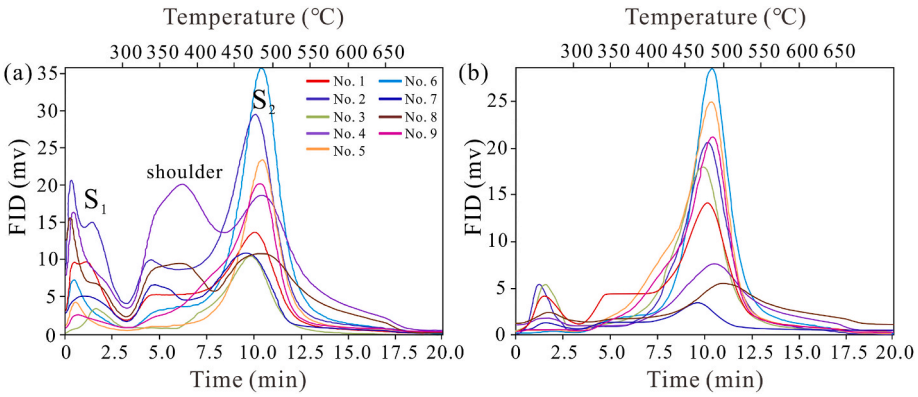

Fig. 3. The Rock–Eval pyrograms for cutting samples before (a) and after (b) extraction, showing a shoulder peak on the left of the S_2 peak in the unextracted sample, which is caused by contamination.

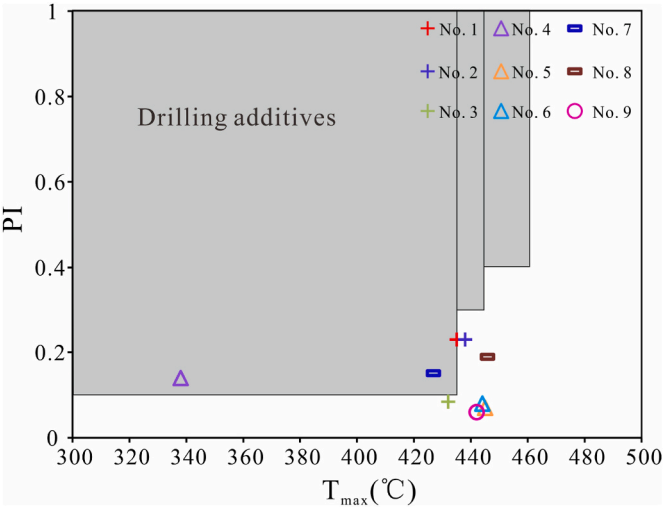

Fig. 4. T_{max}–PI plot for unextracted source rocks of the Wenchang Formation of the Zhu I Depression (after Peters et al., 2005).

Yuan et al., 2021), indicating minor contamination. However, the corresponding "enclosed" bitumen does not have this anomalous distribution, indicating lesser or no contamination. Data for "enclosed" *n*-alkanes are thus more reliable than those of "free" *n*-alkanes for contaminated samples. In addition, the distributions of saturated hydrocarbons in the "enclosed" and "bound" bitumens from contaminated samples also differ (Table 2; Fig. 7), which is consistent with the results for uncontaminated samples.

5.2.1.2. Terpanes and steranes. The *m/z* 191, 217, and 412 mass chromatograms of representative source rock samples are shown in Figs. 6 and 7, illustrating the distributions of tricyclic terpanes, hopanes, C_{27}–C_{29} steranes, C_{30} 4-methylsteranes, and bicadinanes. For uncontaminated samples 3, 5, 6, and 9, the "free", "enclosed", and "bound" bitumens display roughly similar biomarker distributions, even though some biomarker indices differ (Table 2). For example, the three types of bitumen in samples 5 and 6 have high relative abundances of C_{30} 4-methylsteranes and low bicadinane-T contents, whereas these biomarkers are all at low levels in the three bitumens of sample 3. Differences of biomarker ratios among "free", "enclosed", and "bound" bitumens may be related to the state of organic matter in source rocks (Rullkötter and Michaelis, 1990; Kohnen et al., 1991; Love et al., 1995, 1998; Chen and Peng, 2017).

For contaminated samples 1, 2, 4, 7, and 8, the mass chromatograms of "free" and "enclosed" bitumens (Fig. 7) display relatively small differences, implying that contamination has a minor impact on the molecular composition of "free" bitumen studied here. However, differences between "free" and "enclosed" bitumens cannot be ignored when the sample has been subjected to severe drilling mud contamination (Jiang et al., 2021). In view of the effects of contamination, biomarker data for "free" bitumen in contaminated samples are not discussed below. The "enclosed" and "bound" bitumens in contaminated samples have similar biomarker distributions, consistent with the results for uncontaminated samples.

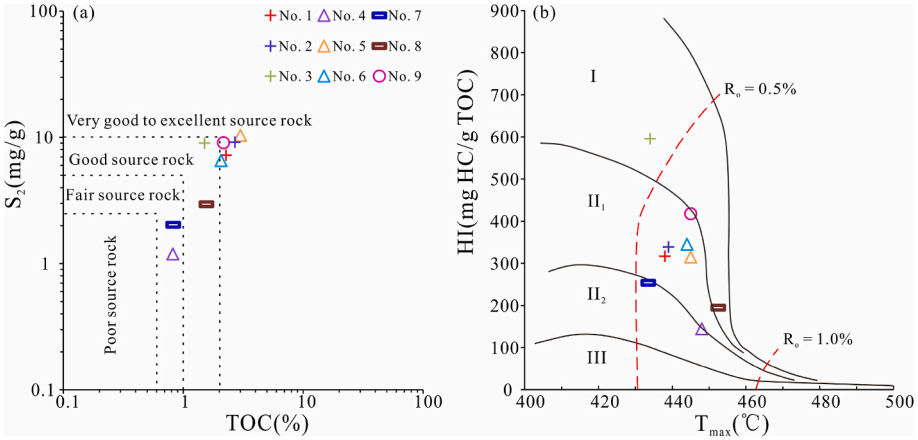

Fig. 5. Cross-plots of S_2 vs. TOC (a) and HI vs. T_{max} (b) for extracted source rocks of the Wenchang Formation of the Zhu I Depression.

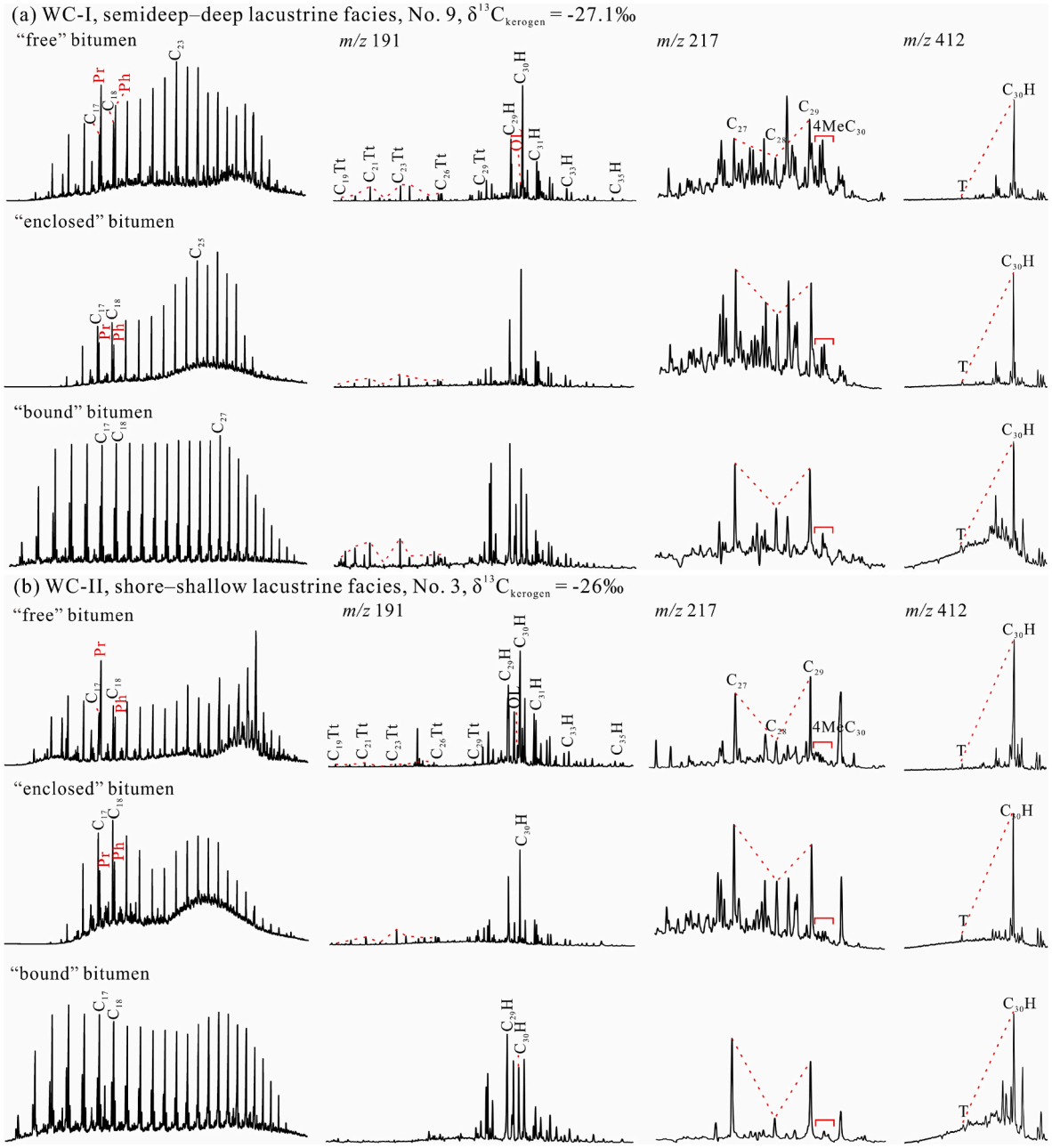

Fig. 6. TIC and mass chromatograms of terpanes (*m/z* 191), steranes (*m/z* 217), and bicadinanes (*m/z* 412) in saturated hydrocarbon fractions from uncontaminated Wenchang Formation source rocks. C_i Tt, C_i tricyclic terpane; $C_{29}H$, 17α(H), 21β(H)-30-norhopane; OL, oleanane; $C_{30}H$, C_{30} 17α(H), 21β(H)-hopane; $C_{31\sim35}H$, $C_{31\sim35}$17α(H), 21β(H)-homohopanes (22S and 22R); C_{27}–C_{29}, C_{27}–C_{29}ααα 20R; T, bicadinane-T.

5.2.2. *Carbon isotopic compositions*

The carbon isotopic distribution profiles of individual *n*-alkanes are shown in Figs. 8 and 9. The $\delta^{13}C$ values of individual *n*-alkanes of "free" and "enclosed" bitumens in uncontaminated samples are very similar (usually within <1‰), but are obviously different to those of corresponding "bound" bitumen, with an offset of >1‰ for most carbon numbers. For example, the $\delta^{13}C$ values of individual *n*-alkanes of "free" and "enclosed" bitumens in sample 5 are similar, generally in the range of −31‰ to −29‰, but the $\delta^{13}C$ values of "bound" *n*-alkanes range from −29‰ to −27‰ (Fig. 8a). Previous studies have suggested that factors such as thermal maturation, organic matter sources, isotopic fractionation during diagenesis, and other secondary alterations may account for differences in the $\delta^{13}C$ values of *n*-alkanes of the different bitumens (Freeman et al., 1990; Clayton, 1991; Boreham et al., 1994; Eglinton, 1994; Love et al., 1998; Xiong and Geng, 2000). Cheng et al. (2015) found that average $\delta^{13}C_{n\text{-alkanes}}$ values of Wenchang Fm. source rocks from the western PRMB increase with thermal maturity. However, maturity parameters, such as 20S/(20S + 20R) and αββ/(ααα + αββ) for the C_{29} steranes, indicate that "bound" bitumen has lower or similar maturity compared with that of corresponding "free" and "enclosed" bitumens (Table 2), so the discrepancies may be attributable to factors such as diagenesis and other secondary alterations rather than thermal maturity. Furthermore, "bound" and corresponding "enclosed" *n*-alkanes in contaminated samples have $\delta^{13}C$ values with offsets of >1‰, consistent with the results for uncontaminated samples (Figs. 8 and 9).

As shown in Fig. 9a, it seems that the carbon isotopic compositions of "free" *n*-alkanes could be divided into two types, but some of the *n*-alkanes were contaminated as demonstrated above (see 5.1 and 5.2

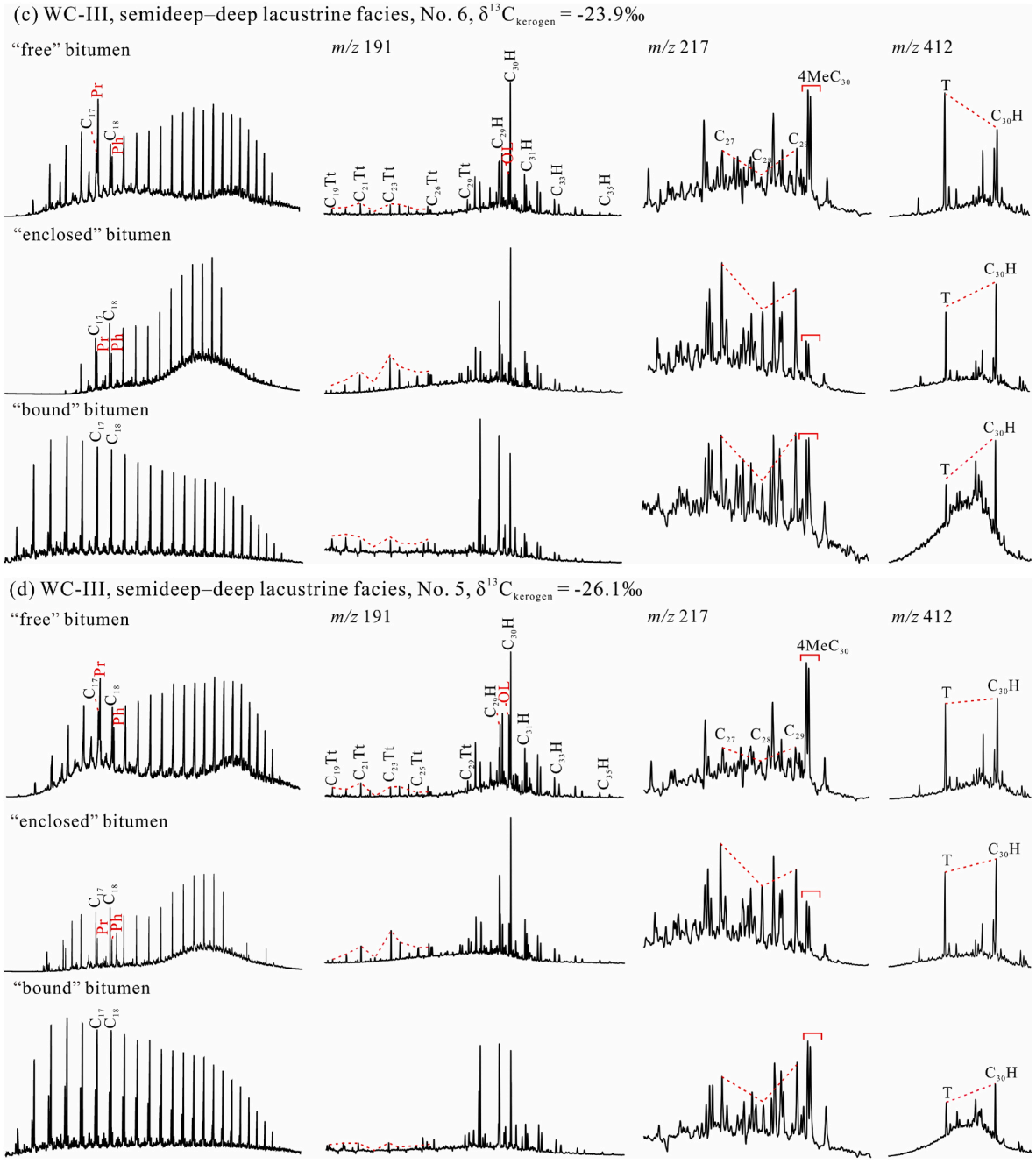

Fig. 6. (*continued*).

section), and further discussion about these results is pointless. In addition, the carbon isotope profiles of "bound" *n*-alkanes may better distinguish different types of source rock than those of "enclosed" *n*-alkanes (Fig. 9b and c). This may be due to the "enclosed" *n*-alkanes being more susceptible to the effects of maturity, which may result in homogenization of the $\delta^{13}C$ values of individual *n*-alkanes with reduction in $\delta^{13}C$ differences among source rocks (Clayton and Bjorøy, 1994).

In summary, "free" and "enclosed" bitumens have similar biomarker distributions and carbon isotopic compositions in uncontaminated samples, so the organic geochemistry of source rocks can be described on the basis of "enclosed" bitumen when the "free" bitumen is contaminated. However, "bound" bitumen is protected by the macromolecular network structure in kerogen and is less affected by diagenetic processes and secondary alteration, so it may provide information on the original source-rock parent material. Characteristics of "bound" bitumen, particularly its carbon isotopic composition, are therefore applied in the following discussions.

5.3. Sedimentary environments and origin of source rocks

According to biomarker characteristics and carbon isotopic compositions of "bound" bitumen, the studied source rocks can be classified into three different types, namely normal medium–deep (WC–I), shore–shallow (WC-II), and special medium–deep (with different algal blooms growth rates; WC-III) lacustrine source rocks (Figs. 6, 7 and 9c), as follows.

The WC-I type source rocks, collected from the Panyu 4 Sag (sample 9), have moderate abundances of C_{30} 4-methylsteranes (4-Me/C_{29} = 0.26) and ultra-low contents of bicadinanes (T/$C_{30}H$ = 0.07; Table 2; Fig. 6). The C_{30} 4-methylsteranes generally originate from

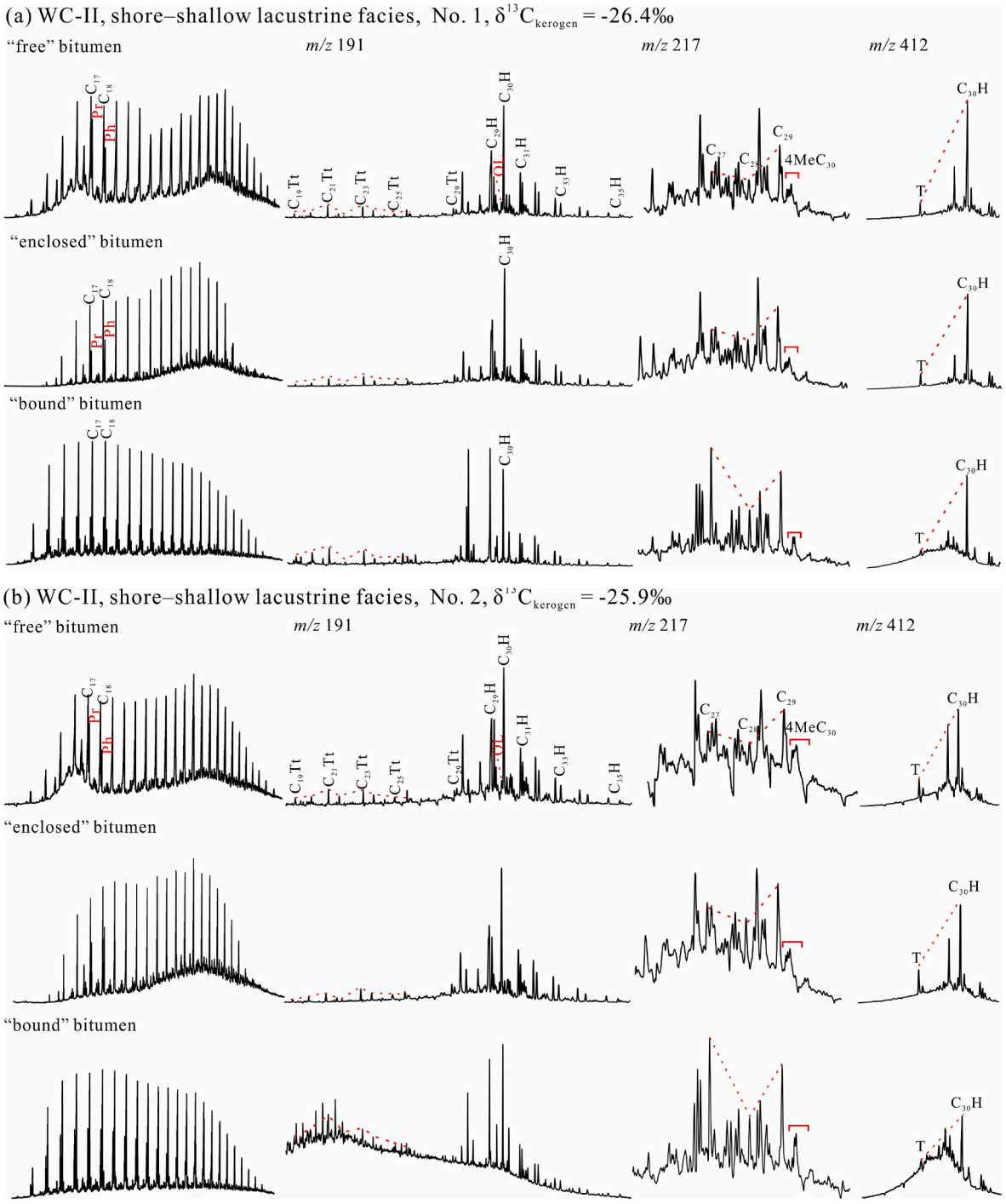

Fig. 7. TIC and mass chromatograms of terpanes (*m/z* 191), steranes (*m/z* 217), and bicadinanes (*m/z* 412) in saturated hydrocarbon fractions from contaminated Wenchang Formation source rocks.

dinoflagellates, prymnesiophyte microalgae, or specific bacteria (Moldowan et al., 1985; Wolff et al., 1986; Summons et al., 1987; Volkman et al., 1990). According to previous researches, the C_{30} 4-methylsteranes are diagnostic biomarkers for lacustrine oils of PRMB, which may be in connection with certain fresh to brackish water dinoflagellates (Brassell et al., 1986; Fu et al., 1993). Bicadinanes are typically derived from terrestrial higher plants (Cox et al., 1986; van Aarssen et al., 1990a, 1990b). WC-I therefore has a relatively predominant aquatic organism input and a minor higher-plant input. The "V-shaped" distribution ($C_{27} \approx C_{29} > C_{28}$) characteristic of C_{27}–C_{29} regular steranes in the WC-I type source rocks (Fig. 6a) also supported the above results. As C_{27} steranes are derived mainly from phytoplankton, whereas C_{29} steranes are mainly related to terrestrial plants and some strains of brown and green algae (Grantham, 1986; Volkman, 1986, 2003; Grantham and Wakefield, 1988). The C_{21} tricyclic terpanes (C_{21}TT) is dominant in freshwater lake source rocks and their related crude oils (Aquino Neto et al., 1983; Ekweozor and Strausz, 1983). The C_{19} and C_{20} tricyclic terpanes (C_{19}–C_{20}TT) are generally reflect the terrestrial organic matter input (Aquino Neto et al., 1983; Hanson et al., 2000). The WC-I has relatively high value of C_{21}/C_{23}TT (2.23) and low ratio of [(C_{19}+C_{20})/C_{23}TT] (2.44) among all the studied samples, indicating them deposited in a freshwater sedimentary environment with a little terrigenous plants

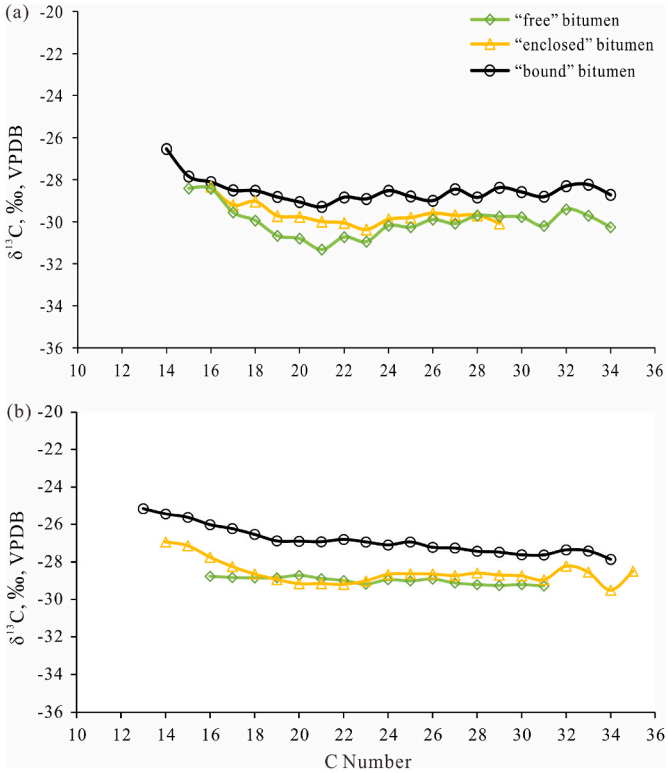

Fig. 8. $\delta^{13}C$ value vs. carbon-number plots for *n*-alkanes in "free", "enclosed", and "bound" bitumens in samples 5 (a) and 1 (b).

input. The low Pr/Ph ratio (1.05) of the WC-I type source rocks reflect an anoxic sedimentary environment (Didyk et al., 1978; Powell, 1988). It is also supported by its relatively high $C_{35}H/C_{34}H$ 22S values (0.84), as the high C_{35}-homohopane indices commonly indicate an anoxic condition (Peters and Moldowan, 1991; Sinninghe Damsté et al., 1995). Furthermore, the WC-I type has the lightest carbon isotopic composition, with the $\delta^{13}C$ values of individual *n*-alkanes ranging from −33‰ to −30‰, with a slightly negative-sloping profile (Fig. 9c), similar to the isotopic compositions of individual *n*-alkanes formed in lacustrine settings (Murray et al., 1994). These characteristics are also consistent with the deposition background: as the lake basin expanded, the water deepened sharply, with development of medium and deep lacustrine grey–brown mudstone (Zhang et al., 2020). The WC-I type source rocks were thus deposited in relatively anoxic, normal medium–deep lacustrine settings with a predominantly aquatic algae and a minor terrigenous plants input.

The WC-II type source rocks, containing samples 1, 2, 3, 4, 7, and 8 from Lufeng, Huizhou, and Xijiang sags, have low contents of C_{30} 4-methylsteranes (4-Me/C_{29} = 0.02–0.22; average 0.10), meaning less input of aquatic organism (Brassell et al., 1986; Fu et al., 1993). In contrast, they are characterized by low to high abundances of bicadinanes ($T/C_{30}H$ = 0.01–1.01; average 0.37), high relative abundances of C_{29} to C_{27}–C_{29} regular steranes (35%–73%; average 50%), medium contents of $C_{21}TT$ ($C_{21}/C_{23}TT$ = 1.10–1.66; average 1.34), high ratios of [(C_{19}+C_{20})/$C_{23}TT$] (1.61–5.06; average 3.45), indicating a high contribution of terrigenous higher plants (Aquino Neto et al., 1983; Ekweozor and Strausz, 1983; Hanson et al., 2000). They have relatively low Pr/Ph (0.65–1.61; average 0.96) and $C_{35}H/C_{34}H$ 22S ratios (0.30–0.82; average 0.55), implying formed in a suboxic conditions (Didyk et al., 1978; Powell, 1988; Sinninghe Damsté et al., 1995). Moreover, they have relatively heavy carbon isotopic compositions, with $\delta^{13}C$ values of individual *n*-alkanes ranging from −29‰ to −26‰, with slightly negative-sloping or almost flat profiles (Fig. 9c), indicating mixed organic material input (Monson and Hayes, 1982; Murray et al., 1994). Average $\delta^{13}C$ values (Table 2) of "bound" *n*-alkanes in the WC-II type source rocks are consistent with those of kerogens (−28.8‰ to −27.1‰) from Wenchang Fm. shore–shallow lacustrine source rocks in the Zhu III Depression of the PRMB (Huang et al., 2003). These characteristics thus suggest that WC-II source rocks were deposited in anoxic to suboxic shore–shallow lacustrine conditions with mixed organic-matter input.

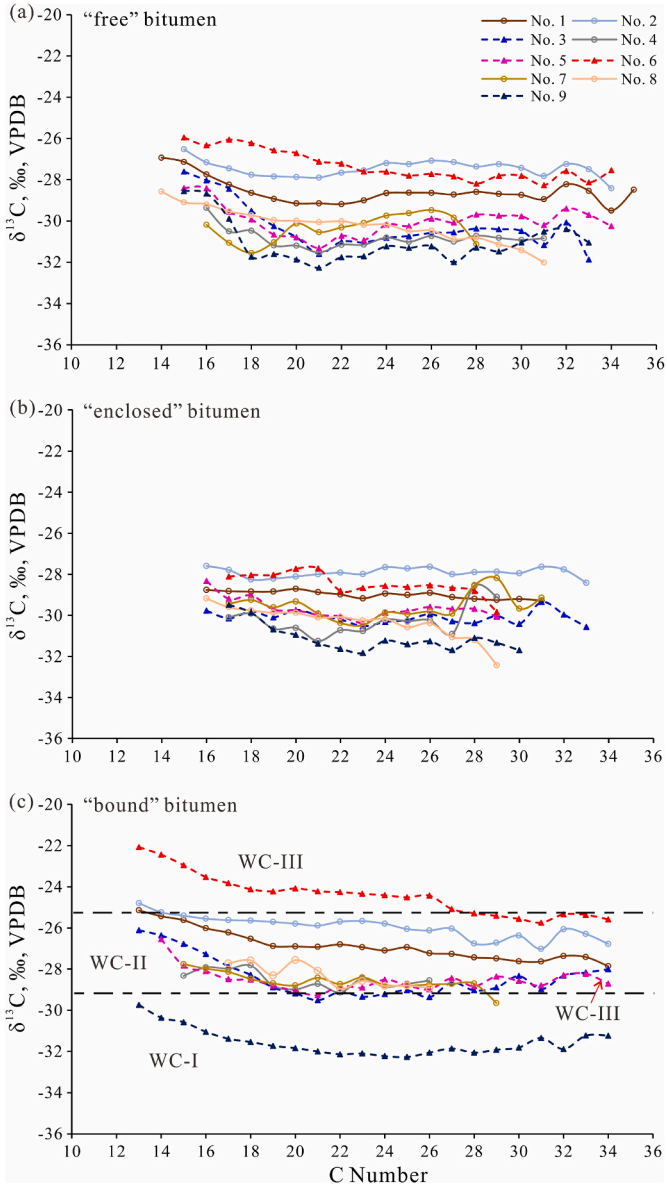

Fig. 9. $\delta^{13}C$ value vs. carbon-number plots for *n*-alkanes in "free" (a), "enclosed" (b), and "bound" (c) bitumens of the Wenchang Formation source rocks.

The WC-III type source rocks from the Huizhou Sag (samples 5 and 6) have high values of 4-Me/C_{29} ratios (0.66–0.77; average 0.71) and "V-shaped" distribution patterns of C_{27}–C_{29} regular steranes (Fig. 6c and d), indicating relatively high contributions of aquatic algae (Moldowan et al., 1985; Brassell et al., 1986; Grantham, 1986; Volkman, 1986, 2003). They also have low contents of bicadinanes ($T/C_{30}H$ < 0.8), moderate values of $C_{21}/C_{23}TT$ (1.10–1.81; average 1.46), and low contents of C_{19} and C_{20} tricyclic terpanes (1.43–1.59; average 1.51), which are similar to that of WC-I, reflecting minor contributions of organic material from land plants. Furthermore, they have low Pr/Ph ratios (0.93–1.07; average 1.00) and relatively high values of $C_{35}H/C_{34}H$ 22S

(0.68–0.70; average 0.69), indicating an anoxic lacustrine environment (Didyk et al., 1978; Powell, 1988; Sinninghe Damsté et al., 1995). However, the $\delta^{13}C$ values of individual *n*-alkanes are heavy and have a relatively wide range of −29‰ to −23‰, consistent with the average $\delta^{13}C$ values of *n*-alkanes in medium–deep lacustrine crude oils (−29.5‰ to −25.4‰) from the Huizhou Sag (Ma et al., 2012). Grice et al. (1998) indicated that the desmethylsteranes with a wide range of $\delta^{13}C$ values (−31.3‰ ~ −23.1‰) might be attribute to diverse algal sources and/or different algae bloom periods with different algae growth rates. Gonçalves (2002) suggested that the $\delta^{13}C$ values (−30‰ ~ −23‰) of the Rio de Contas Formation are mainly related to unusually high rates of primary production. Although the WC-III has similar biomarker characteristics, their $\delta^{13}C$ values display significant differences, indicating that this difference may be caused by other factors rather than their parent material. Moreover, previous studies suggested that the heavy carbon isotopic compositions of source rock and oil in Zhu I Depression is in connection with algal blooms (Huang et al., 2003; Zhang et al., 2003). Therefore, the relatively heavy and widely ranged carbon isotopic compositions for the WC-III type source rocks may be attributable to variable rates of primary productivity in algal blooms. Hence, it might not be reliable for the evaluation of organic-matter origin and the sedimentary environment of source rocks based on biomarker components or carbon isotopic composition alone.

Furthermore, the WC-III type medium–deep lacustrine source rocks differ from the WC-I type, with the former having more abundant C_{30} 4-methylsteranes and heavier isotopic compositions than the latter, which is possibly attributable to high primary productivity with significant aquatic algae input. We therefore speculate that the WC-III type source rocks formed in special medium–deep lacustrine settings, with different algal growth rates.

6. Conclusions

Based on biomarkers and carbon isotopic compositions of “free”, “enclosed”, and “bound” bitumens from Wenchang Formation source rocks in the Zhu I Depression of the PRMB, the main conclusions drawn are as follows.

The Wenchang Formation source rocks have relatively high hydrocarbon potential with relatively high TOC and type II kerogen. “Free” bitumen can be replaced by “enclosed” bitumen for oil–source correlations when being contaminated, as they have very similar biomarker distributions and carbon isotopic compositions. “Bound” bitumen is more representative of the original geochemical characteristics of source rocks.

Three types of source rock from the Wenchang Fm. in the Zhu I Depression were identified according to biomarkers and carbon isotopic compositions. The WC-I type has higher aquatic algae input and the lightest *n*-alkane $\delta^{13}C$ values among the three types of source rock. The WC-III type has high abundances of C_{30} 4-methylsteranes with a wide range of $\delta^{13}C$ values, possibly reflecting different growth rates during algal blooms. The WC-II type has mixed organic-matter input and medium $\delta^{13}C$ values of *n*-alkanes.

The comparative study of “free”, “enclosed”, and “bound” hydrocarbons is not only helpful in providing comprehensive geochemical information for source rocks, especially for samples contaminated by OBM, but also suggesting new view for future oil–source correlations.

Declaration of competing interest

The authors declare that they have no known competing financial interests or personal relationships that could have appeared to influence the work reported in this paper.

Acknowledgments

This study was funded by the Natural Science Foundation of Guangdong Province (Grant No. 2018B030306006), the National Natural Science Foundation of China (Grant Nos. 41902129 and 41773034), the Guangdong Basic and Applied Basic Research Foundation (Grant No. 2019A1515011913), and the Youth Innovation Promotion Association CAS (Grant No. 2018386). We would like to thank the Shenzhen Branch of China National Offshore Oil Corporation Ltd for providing samples and permission to publish this work. This is contribution No. IS-3215 from GIGCAS. We really appreciate Associate Editor and two reviewers for their helpful comments and suggestions which substantially improved our manuscript.

References

Aquino Neto, F.R., Trendel, J.M., Restle, A., Connan, J., Albrecht, P.A., 1983. Occurrence and formation of tricyclic and tetracyclic terpanes in sediments and petroleums. In: Bjorøy, M., et al. (Eds.), Advances in Organic Geochemistry 1981. John Wiley and Sons, pp. 659–667.

Bao, X., Ji, Y., Hu, Y., Zong, Y., 2017. Geochemical characteristics, origins, and model of lacustrine source rocks in the Zhu 1 depression, eastern Pearl River Mouth Basin, South China Sea. AAPG (Am. Assoc. Pet. Geol.) Bull. 101, 1543–1564.

Behar, F., Valérie, B., Penteado, H., 2001. Rock-eval 6 technology: performances and developments. Oil Gas Sci. Technol. 56 (2).

Blumer, M., Thomas, D., 1965. Phytadienes in zooplankton. Science 147, 1148–1149.

Boreham, C.J., Summons, R.E., Roksandic, Z., Dowling, L.M., Hutton, A.C., 1994. Chemical, molecular and isotopic differentiation of organic facies in the tertiary lacustrine Duaringa oil-shale deposit, Queensland, Australia. Org. Geochem. 21, 685–712.

Brassell, S.C., Eglinton, G., Fu, J., 1986. Biological marker compounds as indicators of depositional history of the Maoming oil shale. In: Leythauser, D., Rullkotter, J. (Eds.), Advances in Organic Geochemistry 1985. Organic Geochemistry, vol. 10, pp. 927–941.

Brooks, J.D., Smith, J.W., 1969. The diagenesis of plant lipids during the formation of coal, petroleum and natural gas—II. Coalification and the formation of oil and gas in the Gippsland Basin. Geochem. Cosmochim. Acta 33, 1183–1194.

Caenn, R., Chillingar, G.V., 1996. Drilling fluids: state of the art. J. Petrol. Sci. Eng. 14, 221–230.

Carvajal-Ortiz, H., Gentzis, T., 2015. Critical considerations when assessing hydrocarbon plays using Rock–Eval pyrolysis and organic petrology data: data quality revisited. Int. J. Coal Geol. 152, 113–122.

Chen, J., Peng, P.A., 2017. A comparative study of free and bound bitumens from different mature source rocks with Type III kerogens. Org. Geochem. 112, 1–15.

Chen, S., Zhang, M., Zhang, J., 1991. Study on oil and gas generation and exploration in eastern Pearl River Mouth Basin. Oil Gas Geol. 12, 95–106 (in Chinese with English Abstract).

Chen, S.Z., Pei, C.M., 1993. Geology and geochemistry of source rocks of the eastern Pearl River Mouth Basin, south China sea. J. Southeast Asian Earth Sci. 8, 393–406.

Cheng, P., Xiao, X.M., Gai, H.F., Li, T.F., Zhang, Y.Z., Huang, B.J., Wilkins, R.W.T., 2015. Characteristics and origin of carbon isotopes of n-alkanes in crude oils from the western Pearl River Mouth Basin, South China sea. Mar. Petrol. Geol. 67, 217–229.

Clayton, C.J., 1991. Effect of maturity on carbon isotope ratios of oils and condensates. Org. Geochem. 17, 887–899.

Clayton, C.J., Bjorøy, M., 1994. Effect of maturity on 12C/13C ratios of individual compounds in North Sea oils. Org. Geochem. 21, 737–750.

Cox, H.C., de Leeuw, J.W., Schenck, P.A., van Koningsveld, H., Jansen, J.C., van de Graaf, B., van Geerestein, V.J., Kanters, J.A., Kruk, C., Jans, A.W.H., 1986. Bicadinane, a C30 pentacyclic isoprenoid hydrocarbon found in crude oil. Nature 319, 316–318.

Didyk, B.M., Simoneit, B.R.T., Brassell, S.C., 1978. Organic geochemical indicators of palaeoenvironmental conditions of sedimentation. Nature 272, 216–222.

Duarte, A.C.R., Ribeiro, P.R., Kim, N.R., Mendes, J.R.P., Policarpo, N.A., Vianna, A.M., 2021. An experimental study of gas solubility in glycerin based drilling fluid applied to well control. J. Petrol. Sci. Eng. 207, 109194.

Eglinton, T.I., 1994. Carbon isotopic evidence for the origin of macromolecular aliphatic structures in kerogen. Org. Geochem. 21, 721–735.

Ekweozor, C.M., Strausz, O.P., 1983. Tricyclic terpanes in the Athabasca oil sands: their geochemistry. In: Bjorøy, M., et al. (Eds.), Advances in Organic Geochemistry 1981. John Wiley and Sons, pp. 746–766.

Farrimond, P., Love, G.D., Bishop, A.N., Innes, H.E., Watson, D.F., Snape, C.E., 2003. Evidence for the rapid incorporation of hopanoids into kerogen. Geochem. Cosmochim. Acta 67, 1383–1394.

Freeman, K., Hayes, J., Trendel, J., Albrecht, P., 1990. Evidence from GC–MS carbon-isotopic measurements for multiple origins of sedimentary hydrocarbons. Nature 343, 254–256.

Fu, J., Chen, C., Li, M., Zhang, Z., Long, Z., Wang, T., Lu, X., 2020. Petroleum charging history of neogene reservoir in the Baiyun sag, Pearl River Mouth Basin, south China sea. J. Petrol. Sci. Eng. 190, 106945.

Fu, J., Pei, C., Sheng, G., Liu, D., Chen, S., 1993. A geochemical investigation of crude oils from eastern Pearl River Mouth Basin, south China sea. Southeast Asian Earth Sci. 8, 469–486.

Fu, J., Zhang, Z.T., Chen, C., Wang, T.G., Li, M.J., Ali, S., Lu, X.L., Dai, J.H., 2019. Geochemistry and origins of petroleum in the neogene reservoirs of the Baiyun sag, Pearl River Mouth Basin. Mar. Petrol. Geol. 107, 127–141.

Fu, N., Li, Y.C., Wang, J.R., 2001. Oli-source correlation in the western Huizhou sag. China Offshore Oil Gas 15, 321–328 (in Chinese with English Abstract).
Fu, N., Zhu, L., 2007. Research on mixed oil in western Huizhou sag of Zhu I depression. China Petrol. Explor. 12, 20–26 (in Chinese with English Abstract).
Gabrielle, M.A., Irineu, P.J., 2021. Microwave remediation of oil-contaminated drill cuttings – a review. J. Petrol. Sci. Eng. 207, 109137.
Gonçalves, F.T.T., 2002. Organic and isotope geochemistry of the Early Cretaceous rift sequence in the Camamu Basin, Brazil: paleolimnological inferences and source rock models. Org. Geochem. 33, 67–80.
Grantham, P.J., 1986. The occurrence of unusual C_{27} and C_{29} sterane predominances in two types of Oman crude oil. Org. Geochem. 9, 1–10.
Grantham, P.J., Wakefield, L.L., 1988. Variations in the sterane carbon number distributions of marine source rock derived crude oils through geological time. Org. Geochem. 12, 61–73.
Grice, K., Schouten, S., Peters, K.E., Sinninghe Damsté, J.S., 1998. Molecular isotopic characterisation of hydrocarbon biomarkers in Palaeocene–Eocene evaporitic, lacustrine source rocks from the Jianghan Basin, China. Org. Geochem. 29, 1745–1764.
Hanson, A.D., Zhang, S.C., Moldowan, J.M., Liang, D.G., Zhang, B.M., 2000. Molecular organic geochemistry of the Tarim basin. Northwest China Am. Assoc. Petrol. Geol. Bull. 84, 1109–1128.
Hu, Y., Hao, F., Zhu, J., 2015. Origin and occurrence of crude oils in the Zhu I sub-basin, Pearl River Mouth Basin, China. J. Asian Earth Sci. 97, 24–37.
Huang, B., Xiao, X., Zhang, M., 2003. Geochemistry, grouping and origins of crude oils in the western Pearl River Mouth Basin, offshore south China sea. Org. Geochem. 34, 993–1008.
Huang, Z.J., 1998. Nonmarine source rock and petroleum Formation of Pearl River Mouth Basin. China Offshore Oil Gas 12, 255–261 (in Chinese with English Abstract).
Jarvie, D.M., 2012. Shale resource systems for oil and gas: part 2—shale–oil resource systems. In: Breyer, J.A. (Ed.), Shale Reservoirs—Giant Resources for the 21st Century. AAPG Memoir 97 142, pp. 89–119.
Jiang, H., Pang, X., Shi, H., Yu, Q., Cao, Z., Yu, R., Chen, D., Long, Z., Jiang, F., 2015. Source rock characteristics and hydrocarbon expulsion potential of the Middle Eocene Wenchang formation in the Huizhou depression, Pearl River Mouth basin, south China sea. Mar. Petrol. Geol. 67, 635–652.
Jiang, W., Li, Y., Yang, C., Xiong, Y., 2021. Organic geochemistry of source rocks in the Baiyun sag of the Pearl River Mouth Basin, south China sea. Mar. Petrol. Geol. 124, 104836.
Kohnen, M.E.L., Sinninghe Damste, J.S., De Leeuw, J.W., 1991. Biases from natural sulphurization in palaeoenvironmental reconstruction based on hydrocarbon biomarker distributions. Nature 349, 775–778.
Lafargue, E., Marquis, F., Pillot, D., 1998. Rock-eval 6 applications in hydrocarbon exploration, production, and soil contamination studies. Revue de l'Institut Français du Pétrole, EDP Sciences 53 (4), 421–437.
Liao, Y., Fang, Y., Wu, L., Geng, A., Hsu, C.S., 2012. The characteristics of the biomarkers and δ13C of n-alkanes released from thermally altered solid bitumens at various maturities by catalytic hydropyrolysis. Org. Geochem. 46, 56–65.
Li, P.L., Rao, C.T., 1994. Tectonic characteristics and evolution history of the Pearl River Mouth Basin. Tectonophysics 235, 13–25.
Love, G., Snape, C.E., Carr, A.D., Houghton, R.C., 1996. Changes in molecular biomarker and bulk carbon skeletal parameters of vitrinite concentrates as a function of rank. Energy Fuel. 10, 149–157.
Love, G.D., McAulay, A., Snape, C.E., Bishop, A.N., 1997. Effect of process variables in catalytic hydropyrolysis on the release of covalently bound aliphatic hydrocarbons from sedimentary organic matter. Energy Fuel. 11, 522–531.
Love, G.D., Snape, C.E., Carr, A.D., Houghton, R.C., 1995. Release of covalently-bound alkane biomarkers in high yields from kerogen via catalytic hydropyrolysis. Org. Geochem. 23, 981–986.
Love, G.D., Snape, C.E., Fallick, A.E., 1998. Differences in the mode of incorporation and biogenicity of the principal aliphatic constituents of a Type I oil shale. Org. Geochem. 28, 797–811.
Ma, N., Hou, D.J., Shi, H.S., 2012. Study on oil genesis in Huizhou depression. Fault-Block Oil Gas Field 19, 545–549 (in Chinese with English Abstract).
Marzi, R., Torkelson, B.E., Olson, R.K., 1993. A revised carbon preference index. Org. Geochem. 20, 1303–1306.
McDermott, J., 1973. Drilling Mud and Fluid Additive. Noyes Data Corporation, Park Ridge, New Jersey, p. 336.
Meredith, W., Russell, C.A., Cooper, M., Snape, C.E., Love, G.D., Fabbri, D., Vane, C.H., 2004. Trapping hydropyrolysates on silica and their subsequent thermal desorption to facilitate rapid fingerprinting by GC–MS. Org. Geochem. 35, 73–89.
Meredith, W., Snape, C., Love, G., 2015. Development and use of catalytic hydropyrolysis (HyPy) as an analytical tool for organic geochemical applications. In: Principles and Practice of Analytical Techniques in Geosciences. The Royal Society of Chemistry, pp. 171–208.
Meredith, W., Uguna, C., Snape, C., Carr, A., Scotchman, I., 2020. formation of bitumen in the elgin/franklin complex, Central Graben, north sea: implications for hydrocarbon charging. Geol. Soc., Lond., Spec. Publ. 484, 139–163.
Moldowan, J.M., Seifert, W., Gallegos, E., 1985. Relationship between petroleum composition and depositional environment of petroleum source rock. AAPG (Am. Assoc. Pet. Geol.) Bull. 69, 1255–1268.
Monson, K.D., Hayes, J.M., 1982. Biosynthetic control of the natural abundance of carbon 13 at specific positions within fatty acids in Saccharomyces cerevisiae. Isotopic fractionation in lipid synthesis as evidence for peroxisomal regulation. J. Biol. Chem. 257, 5568–5575.
Murray, A.P., Summons, R.E., Boreham, C.J., Dowling, L.M., 1994. Biomarker and N-alkane isotope profiles for tertiary oils-relationship to source-rock depositional setting. Org. Geochem. 22, 521–542.
Murray, I.P., Love, G.D., Snape, C.E., Bailey, N.J.L., 1998. Comparison of covalently-bound aliphatic biomarkers released via hydropyrolysis with their solvent-extractable counterparts for a suite of Kimmeridge clays. Org. Geochem. 29, 1487–1505.
Niu, Z., Liu, G., Ge, J., Zhang, X., Cao, Z., Lei, Y., An, Y., Zhang, M., 2019. Geochemical characteristics and depositional environment of paleogene lacustrine source rocks in the Lufeng sag, Pearl River Mouth Basin, south China sea. J. Asian Earth Sci. 171, 60–77.
Peng, J., Pang, X., Shi, H., Peng, H., Xiao, S., Yu, Q., Wu, L., 2016. Hydrocarbon generation and expulsion characteristics of Eocene source rocks in the Huilu area, northern Pearl River Mouth basin, South China Sea: implications for tight oil potential. Mar. Petrol. Geol. 72, 463–487.
Peters, K.E., Cassa, M.R., 1994. Applied source rock geochemistry. In: Magoon, L.B., Dow, W.G. (Eds.), The Petroleum System–From Source to Trap, vol. 60. AAPG Memoir, pp. 93–120.
Peters, K.E., Moldowan, J.M., 1991. Effects of source, thermal maturity, and biodegradation on the distribution and isomerization of homohopanes in petroleum. Org. Geochem. 17 (1), 47–61.
Peters, K.E., Walters, C.C., Moldowan, J.M., 2005. The Biomarker Guide: Biomarkers and Isotopes in Petroleum Systems and Earth History. Cambridge University Press, Cambridge.
Petersen, H.I., Hertle, M., Sulsbrück, H., 2017. Upper Jurassic–lowermost Cretaceous marine shale source rocks (Farsund Formation), North Sea: kerogen composition and quality and the adverse effect of oil-based mud contamination on organic geochemical analyses. Int. J. Coal Geol. 173, 26–39.
Ping, H.W., Chen, H.H., Zhai, P.Q., Zhu, J.Z., George, S.C., 2019. Petroleum charge history in the Baiyun depression and Panyu lower uplift in the Pearl River Mouth Basin, northern South China Sea: constraints from integration of organic geochemical and fluid inclusion data. AAPG (Am. Assoc. Pet. Geol.) Bull. 103, 1401–1442.
Potts, L.D., Perez Calderon, L.J., Gubry-Rangin, C., Witte, U., Anderson, J.A., 2019. Characterisation of microbial communities of drill cuttings piles from offshore oil and gas installations. Mar. Pollut. Bull. 142, 169–177.
Powell, T., 1988. Pristane/phytane ratio as environmental indicator. Nature 333 (6174), 604-604.
Ratnayake, A.S., Sampei, Y., 2019. Organic geochemical evaluation of contamination tracers in deepwater well rock cuttings from the Mannar Basin, Sri Lanka. J. Pet. Explor. Prod. Technol. 9, 989–996.
Robison, C.R., Elrod, L.W., Bissada, K.K., 1998. Petroleum generation, migration, and entrapment in the Zhu 1 depression, Pearl River Mouth Basin, south China sea. Int. J. Coal Geol. 37, 155–178.
Rodriguez, N.D., Katz, B.J., 2021. The effect of oil-based drilling mud (OBM) on the assessment of hydrocarbon charge potential. Mar. Petrol. Geol. 133, 105312.
Rullkötter, J., Michaelis, W., 1990. The structure of kerogen and related materials. A review of recent progress and future trends. Org. Geochem. 16, 829–852.
Russell, C.A., Snape, C.E., Meredith, W., Love, G.D., Clarke, E., Moffatt, B., 2004. The potential of bound biomarker profiles released via catalytic hydropyrolysis to reconstruct basin charging history for oils. Org. Geochem. 35, 1441–1459.
Seifert, W.K., Moldowan, J.M., 1980. Effect of thermal stress on source-rock quality as measured by hopane stereochemistry. Phys. Chem. Earth 12, 229–237.
Shi, H.S., He, M., Zhang, L.L., Yu, Q.H., Pang, X., Zhong, Z.H., Liu, L.H., 2014. Hydrocarbon geology, accumulation pattern and the next exploration strategy in the eastern Pearl River Mouth Basin. China Offshore Oil Gas 26, 11–22 (in Chinese with English Abstract).
Shi, Y.L., Hou, D.J., Ma, N., 2011. Hydrocarbon-generating potential and correlation of oil sources in Huizhou oil-enriched depression. J. Oil Gas Technol. (J. Jianghan Petroleum Inst.) 33, 15–19 (in Chinese with English Abstract).
Sinninghe Damsté, J.S., Van Duin, A.C.T., Hollander, D., 1995. Early diagenesis of bacteriohopanepolyol derivatives: formation of fossil homohopanoids. Geochem. Cosmochim. Acta 59, 5141–5157.
Stuckman, M.Y., Lopano, C.L., Berry, S.M., Hakala, J.A., 2019. Geochemical solid characterization of drill cuttings, core and drilling mud from Marcellus Shale Energy development. J. Nat. Gas Sci. Eng. 68, 102922.
Summons, R.E., Volkman, J.K., Boreham, C.J., 1987. Dinosterane and other steroidal hydrocarbons of dinoflagellate origin in sediments and petroleum. Geochem. Cosmochim. Acta 51, 3075–3082.
van Aarssen, B.G.K., Cox, H.C., Hoogendoorn, P., De Leeuw, J.W., 1990a. A cadinene biopolymer in fossil and extant dammar resins as a source for cadinanes and bicadinanes in crude oils from South East Asia. Geochem. Cosmochim. Acta 54, 3021–3031.
van Aarssen, B.G.K., Kruk, C., Hessels, J.K.C., de Leeuw, J.W., 1990b. Cis-cis-trans-bicadinane, a novel member of an uncommon triterpane family isolated from crude oils. Tetrahedron Lett. 31, 4645–4648.
Volkman, J.K., Kearney, P., Jeffrey, S.W., 1990. A new source of 4-methyl sterols and 5α (H)-stanols in sediments: prymnesiophyte microalgae of the genus Pavlova. Org. Geochem. 15, 489–497.
Volkman, J.K., 1986. A Review of Sterol Markers for Marine and Terrigenous Organic Matter Org, vol. 9, pp. 83–99. Geochem.
Volkman, J.K., 2003. Sterols in microorganisms. Appl. Microbiol. Biotechnol. 60 (5), 495–506.
Wang, Q.T., Jiang, L.X., Liu, Q.B., Zeng, J., Lu, H., Liu, J.Z., Peng, P.A., 2012. Catalytic hydropyrolysis for kerogens of middle and upper Ordovician source rocks in keping

section, Tarim basin, Northwestern China. Geochimica 41, 415–424 (in Chinese with English Abstract).
Wolff, G.A., Lamb, N.A., Maxwell, J.R., 1986. The origin and fate of 4-methyl steroids—II. Dehydration of stanols and occurrence of C30 4-methyl steranes. Org. Geochem. 10, 965–974.
Xiong, Y., Geng, A., 2000. Carbon isotopic composition of individual n-alkanes in asphaltene pyrolysates of biodegraded crude oils from the Liaohe Basin, China. Org. Geochem. 31, 1441–1449.
Yuan, L., Jiang, W., Li, Y., Xiong, Y., 2021. Combining catalytic hydropyrolysis and GC–IRMS to reconstruct the geochemical characteristics of source rocks in the Baiyun deep-water area of the Pearl River Mouth Basin, China. Mar. Petrol. Geol. 131, 105166.
Zhang, S., Liang, D., Gong, Z., Wu, K., Li, M., Song, F., Song, Z., Zhang, D., Wang, P., 2003. Geochemistry of petroleum systems in the eastern Pearl River Mouth Basin: evidence for mixed oils. Org. Geochem. 34, 971–991.
Zhang, X.T., Zhu, J.Z., Xiong, W.L., Qin, C.G., 2020. Biomarker characteristics and oil–source discrimination of source rocks in wenchang formation of panyu 4 sag. China Offshore Oil Gas 32, 12–23 (in Chinese with English Abstract).